

2021 ASHRAE HANDBOOK

FUNDAMENTALS

SI Edition

Supported by ASHRAE Research

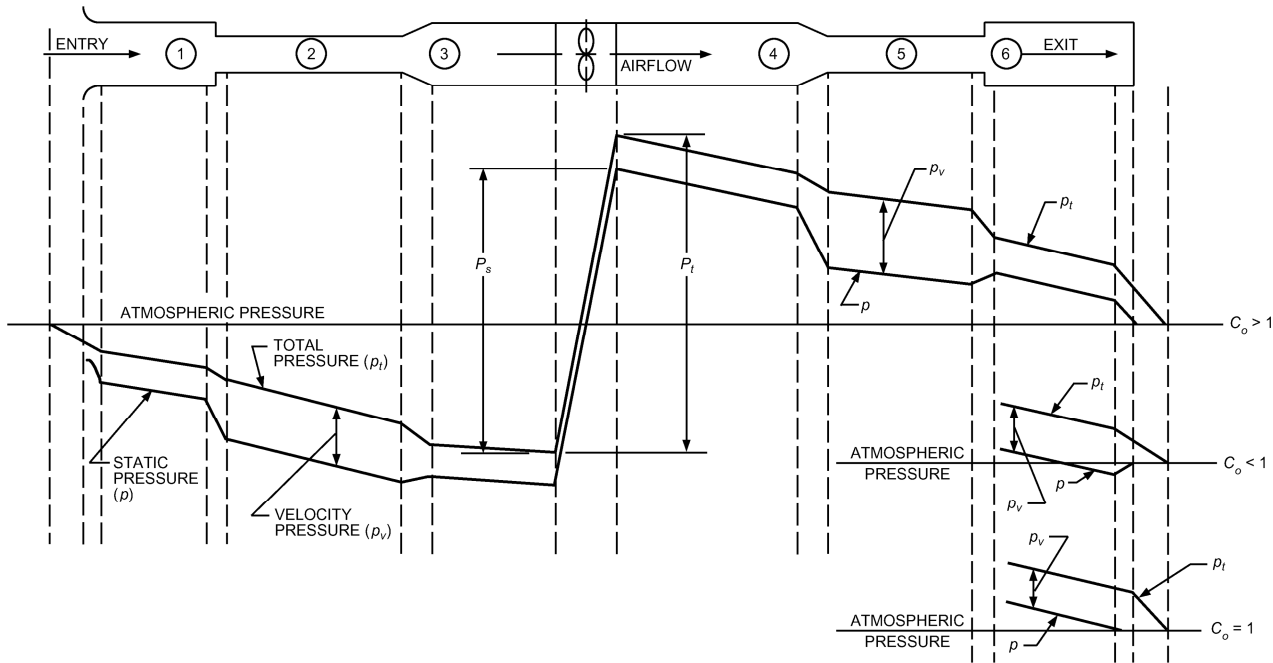


Fig. 6 Pressure Changes During Flow in Ducts

crease. The static pressure increase at these sections is known as **static regain**.

At converging transitions, velocity pressure increases in the direction of airflow, and absolute total and absolute static pressures decrease.

At the exit, total pressure loss depends on the shape of the fitting and the flow characteristics. Exit loss coefficients C_o can be greater than, less than, or equal to one. Total and static pressure grade lines for the various coefficients are shown in Figure 6. Note that, for a loss coefficient less than one, static pressure upstream of the exit is less than atmospheric pressure (negative). Static pressure just upstream of the discharge fitting can be calculated by subtracting the upstream velocity pressure from the upstream total pressure.

At section 1, total pressure loss depends on the shape of the entry. Total pressure immediately downstream of the entrance equals the difference between the upstream pressure, which is zero (atmospheric pressure), and loss through the fitting. Static pressure of ambient air is zero; several diameters downstream, static pressure is negative, equal to the sum of the total pressure (negative) and the velocity pressure (always positive).

System resistance to airflow is noted by the total pressure grade line in Figure 6. Sections 3 and 4 include fan system effect pressure losses. To obtain the fan static pressure rise requirement for selecting fans rated using this parameter (i.e., for fans with unducted outlets, such as plenum fans) and where fan total pressure rise is known, use

$$P_s = P_t - P_{v,o} \quad (17)$$

where

P_s = fan static pressure rise, Pa

P_t = fan total pressure rise, Pa

$P_{v,o}$ = fan outlet velocity pressure, Pa

Fan static pressure rise is also the difference between the fan outlet static pressure and the fan inlet total pressure ($P_{s,o} - P_{t,i}$). However, note that fan static pressure rise is not the difference in static pressure between the fan inlet and fan outlet, nor is it the sum of static pressure differences for components in the air-handling system.

3. FLUID RESISTANCE

Duct system losses are the irreversible transformation of mechanical energy into heat. The two types of losses are (1) friction and (2) dynamic.

3.1 FRICTION LOSSES

Friction losses are caused by shear stresses related to fluid viscosity. They result from adjacent fluid layers moving at different velocities. Turbulence also causes the fluid to transfer momentum, heat, and mass very rapidly across the flow. As a result, fluid velocities of the turbulent profile near the wall must drop to zero more rapidly than those of the laminar profile. In turn, friction losses are much greater in turbulent flow compared to laminar flow. Chapter 3 provides further details about ducted flows and friction losses. Friction losses occur along the entire duct length.

Darcy and Colebrook Equations

For fluid flow in conduits, friction loss can be calculated by the Darcy equation:

$$\Delta p_f = \frac{1000 f L}{D_h} \times \frac{\rho V^2}{2} \quad (18)$$

where

Δp_f = friction losses in terms of total pressure, Pa

f = friction factor, dimensionless

L = duct length, m

D_h = hydraulic diameter [Equation (24)], mm

V = velocity, m/s

ρ = density, kg/m³

In the region of laminar flow (Reynolds numbers less than 2300), the friction factor is a function of Reynolds number only. For completely turbulent flow (fully rough), the friction factor depends on duct surface roughness and internal protuberances (e.g., joints). Between the bounding limits of hydraulically smooth behavior (laminar flow) and fully rough behavior is a transitional zone where the friction factor depends on both roughness and Reynolds number.

In both the transitional and fully rough regions (see Moody diagram: Figure 13 in [Chapter 3](#)), the friction factor f is calculated by Colebrook's equation (Colebrook 1938-1939). Because Colebrook's equation cannot be solved explicitly for f , use iterative techniques to determine f (Behls 1971).

$$\frac{1}{\sqrt{f}} = -2 \log \left(\frac{\epsilon}{3.7D_h} + \frac{2.51}{Re \sqrt{f}} \right) \quad (19)$$

where

ϵ = material absolute roughness factor, mm

Re = Reynolds number

Reynolds number (Re) is calculated using the following equation.

$$Re = \frac{D_h V}{1000 \nu} \quad (20)$$

where ν = kinematic viscosity, m^2/s .

For standard air and temperature between 4 and 38°C, Re can be calculated by

$$Re = 66.4 D_h V \quad (21)$$

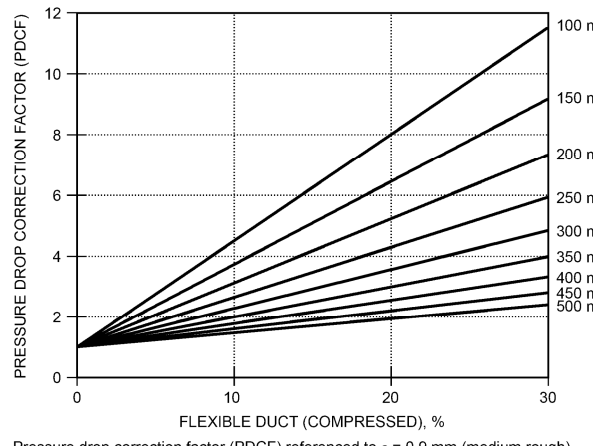
Roughness Factors

Roughness factors listed in [Table 1](#), column 3, are recommended for use with Equation (19). For increased calculation accuracy, use an absolute roughness factor from column 2.

Flexible Duct. For fully stretched and compressed flexible duct, use Equation (22) or [Figure 7](#) (Abushakra et al. 2004; Culp 2011), where the multiplier PDCF is based on flexible duct with an absolute roughness $\epsilon = 0.9$ mm. The resistance of flexible duct can be calculated using Fitting CD11-2 in the *ASHRAE Duct Fitting Database* (ASHRAE 2016). Flexible duct should be installed fully extended; its resistance even when fully extended is approximately 50% more compared to the resistance of an equivalent diameter rigid galvanized-steel spiral duct. See [Example 6](#) for the increase in resistance of flexible duct fully stretched and compressed relative to rigid spiral duct.

For commercial systems, flexible ducts should be

- Limited to connections of rigid ducts to diffusers. For diffuser installation suggestions, see [Figure 8](#). The purpose of limiting the



Pressure drop correction factor (PDCF) referenced to $\epsilon = 0.9$ mm (medium rough) (Abushakra 2004; Culp 2011)

Fig. 7 Pressure Loss Correction Factor for Flexible Duct Not Fully Extended

offset to $D/8$ in [Figure 8B](#) is to minimize noise generation. Flexible duct should not be installed upstream of variable-air-volume (VAV) boxes.

Commentary: The loss coefficient or pressure loss for flexible duct elbows, such as those in [Figure 8A](#), can be obtained from the *ASHRAE Duct Fitting Database* (ASHRAE 2016), Fitting CD3-22 ($r/D = 1.0$) or CD3-23 ($r/D = 1.5$). Loss coefficients are for fully stretched elbows.

- Limited to 2 m maximum, fully stretched.
- Installed without any radial compression.

Example 6. Compare the total pressure resistance of 250 mm, 1.8 m installed length, galvanized steel spiral and flexible duct, 0% compressed (fully stretched), 4%, 15%, and 30% compressed. Airflow is 470 L/s, air density is 1.204 kg/m³, and absolute roughnesses ϵ of spiral round and flexible ducts are 0.12 mm and 0.9 mm. Calculate using the *ASHRAE Duct Fitting Database* [DFDB; ASHRAE (2016)].

Solution: See [Table 2](#) for results.

$$PDCF = 1 + 0.58 K_c e^{-0.00496D} \quad (22)$$

with

$$K_c = \left(\frac{L_{FE} - L}{L_{FE}} \right) 100 \quad (23)$$

where

PDCF = pressure drop correction factor

K_c = flexible duct compressed, percent

D = flexible duct diameter, mm

L = installed duct length, m

L_{FE} = duct length fully extended, m

Friction Chart

The friction chart ([Figure 9](#)) is a plot of the Darcy and Colebrook equations [Equations (18) and (19), respectively], where the absolute roughness is 0.09 mm and the air is standard air (density = 1.204 kg/m³). [Figure 9](#) can be used for (1) duct construction/materials categorized as "average" in [Table 1](#), (2) temperature variations of ± 15 K from 20°C, (3) elevations to 500 m, and (4) duct pressures from -5 to $+5$ kPa relative to ambient pressure. These individual variations in temperature, elevation, and duct pressure result in duct losses within $\pm 5\%$ of the standard air friction chart.

The friction chart was changed in 1985 from an absolute roughness of 0.15 mm to 0.09 mm based on research by Griggs et al. (1987), who found that the roughness factor is affected by the material surface, joint spacing, and type of joint. The Wright friction chart appeared in the Handbook from 1946 to 1981. This chart was based on an absolute roughness $\epsilon = 0.15$ mm, primarily because of the 760 mm joint spacing. In 1985 the friction chart was changed to $\epsilon = 0.09$ mm because joint spacing was increasing. For the relative effect of straight duct resistance between charts, see [Figure 10](#). For a 250 mm diameter duct at 10 m/s (491 L/s), the resistance decreased 5 to 6%.

Noncircular Ducts

A momentum analysis can relate average wall shear stress to pressure drop per unit length for fully developed turbulent flow in a passage of arbitrary shape but uniform longitudinal cross-sectional area. This analysis leads to the definition of **hydraulic diameter**:

$$D_h = 4A/P \quad (24)$$

where

D_h = hydraulic diameter, mm

A = duct area, mm²

P = perimeter of cross section, mm

Although hydraulic diameter is often used to correlate noncircular data, exact solutions for laminar flow in noncircular passages show that this causes some inconsistencies. No exact solutions exist for

Table 1 Duct Roughness Factors

Duct Type/Material	1	2	3
	Range	Absolute Roughness ϵ , mm	
		Roughness Category	
Drawn tubing (Madison and Elliot 1946)	0.00046	Smooth	0.00046
PVC plastic pipe (Swim 1982)	0.009 to 0.046	Medium smooth	0.046
Commercial steel or wrought iron (Moody 1944)	0.046		
Aluminum, round, longitudinal seams, crimped slip joints, 0.91 m spacing (Hutchinson 1953)	0.037 to 0.061		
<i>Friction chart:</i>			
Galvanized steel, round, longitudinal seams, variable joints (Vanstone, drawband, welded. Primarily beaded coupling), 1.22 m joint spacing (Griggs et al. 1987)	0.049 to 0.098	Average	0.09
Galvanized steel, spiral seams, 3.05 m joint spacing (Jones 1979)	0.061 to 0.12		
Galvanized steel, spiral seam with 1, 2, and 3 ribs, beaded couplings, 3.66 m joint spacing (Griggs et al. 1987)	0.088 to 0.116		
Galvanized steel, rectangular, various type joints (Vanstone, drawband, welded. Beaded coupling), 1.22 m spacing ^a (Griggs and Khodabakhsh-Sharifabad 1992)	0.082 to 0.15		
Phenolic duct, aluminum foil on the interior face, sections connected with a four-bolt flange and cleat joint (Idem and Paruchuri 2018)			
1.52 m spacing:	0.149 to 0.391		
3.05 m spacing	0.075 to 0.298		
<i>Wright Friction Chart:</i>			
Galvanized steel, round, longitudinal seams, 0.76 m joint spacing, $\epsilon = 0.15$ mm	Retained for historical purposes [See Wright (1945) for development of friction chart]		
Flexible duct, nonmetallic and wire, fully extended (Abushakra et al. 2004; Culp 2011)	0.09 to 0.9	Medium rough	0.9
Galvanized steel, spiral, corrugated, ^b Beaded slip couplings, 3.05 m spacing (Kulkarni et al. 2009)	0.54 to 0.91		
Fibrous glass duct, rigid (tentative) ^c	—		
Fibrous glass duct liner, air side with facing material (Swim 1978)	1.52		
Fibrous glass duct liner, air side spray coated (Swim 1978)	4.57	Rough	3.0
Flexible duct, metallic corrugated, fully extended	1.2 to 2.1		
Concrete (Moody 1944)	0.30 to 3.0		

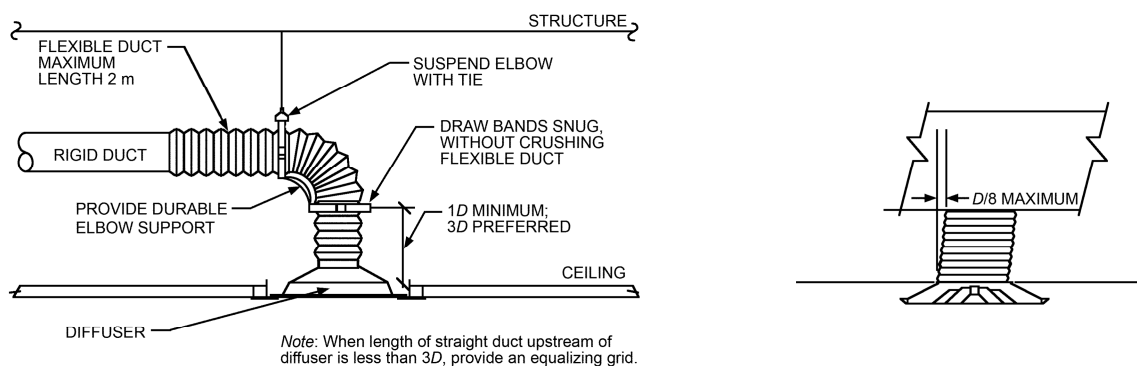
^aGriggs and Khodabakhsh-Sharifabad (1992) showed that ϵ values for rectangular duct construction combine effects of surface condition, joint spacing, joint type, and duct construction (cross breaks, etc.), and that the ϵ -value range listed is representative.

^bSpiral seam spacing was 119 mm with two corrugations between seams. Corrugations were 19 mm wide by 6 mm high (semicircle).

^cSubject duct classified "tentatively medium rough" because no data available.

Table 2 Solution for Example 6

Duct	DFDB Fitting	ϵ , mm	Airflow, L/s	Diameter, mm	Velocity, m/s	Compression, %	PDCF	Δp_r , Pa	% Δp_r Increased
Galvanized steel, spiral	CD11-1	0.12	470	250	9.6	NA	NA	7.7	Base
Flexible	CD11-2	0.9	470	250	9.6	(fully stretched)	1.0	11.4	48
Flexible	CD11-2	0.9	470	250	9.6	4	1.7	19.5	153
Flexible	CD11-2	0.9	470	250	9.6	15	3.5	40.0	419
Flexible	CD11-2	0.9	470	250	9.6	30	5.9	68.9	795



A. DIFFUSER WITH FLEXIBLE DUCT CONNECTION

B. RECTANGULAR HEADER

Fig. 8 Diffuser Installation Suggestions

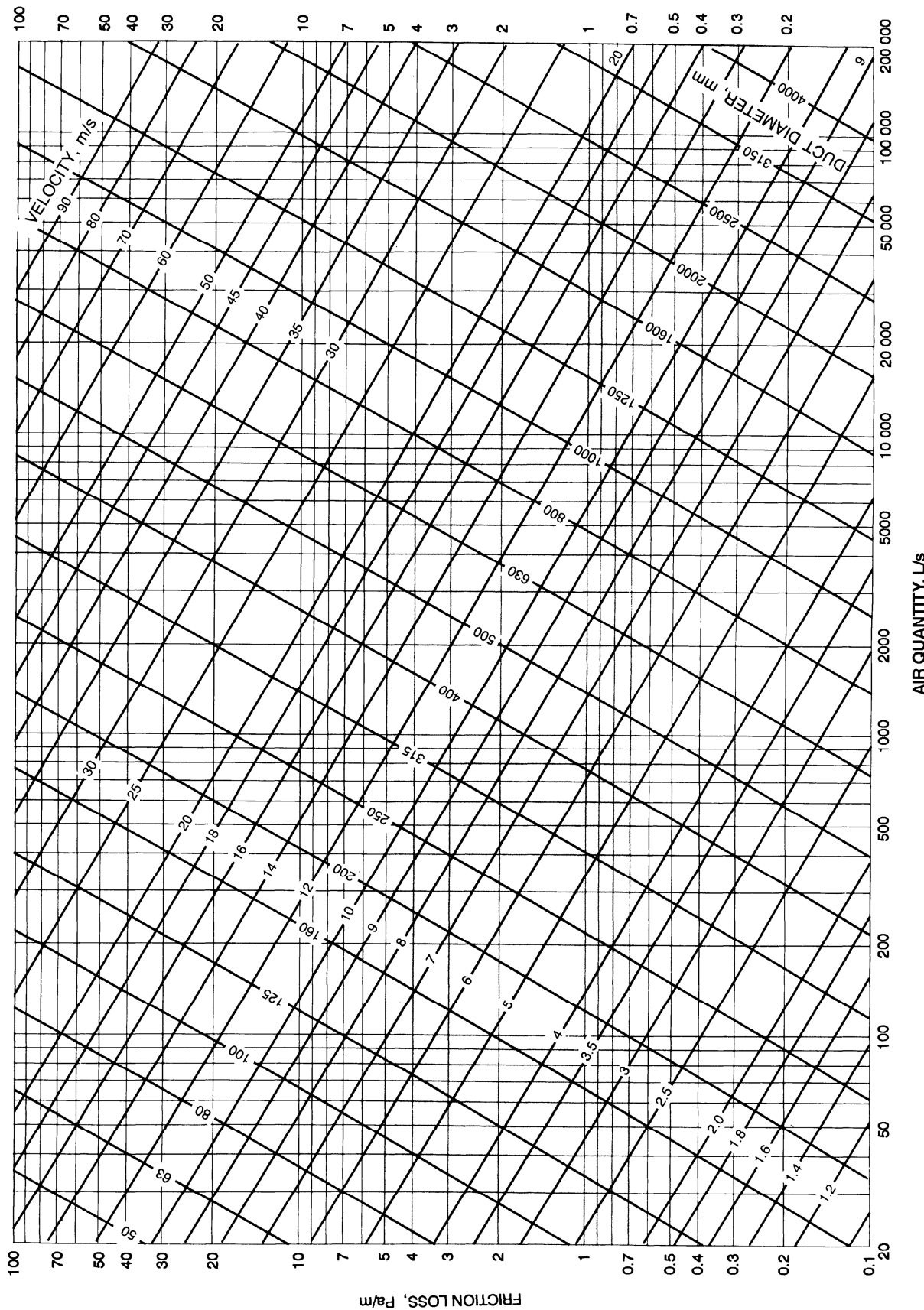


Fig. 9 Friction Chart for Round Duct ($\rho = 1.20 \text{ kg/m}^3$ and $\varepsilon = 0.09 \text{ mm}$)